Proceedings of the 8th International Conference on Gas Hydrates (ICGH8-2014),
Beijing, China, 28 July - 1 August, 2014

Environmental change, hydrate dissociation, and submarine slope failure along continental margins: the role of saturation anomalies in landslide triggering

Alexander L. Handwerger
Department of Geological Sciences, University of Oregon, 1275 E. 13th Ave., Eugene, OR 97403-1272, USA

Alan W. Rempel
Department of Geological Sciences, University of Oregon, 1275 E. 13th Ave., Eugene, OR 97403-1272, USA

ABSTRACT

Submarine landslides occur along active and passive continental margins and are potentially triggered by numerous factors including the dissociation of gas hydrates. The hazard produced by such landslides can damage infrastructure (oil platforms, telecommunication lines), generate tsunamis, and cause a catastrophic release of methane to the atmosphere and ocean. Here we develop numerical models to identify the conditions under which the dissociation of gas hydrates can trigger submarine landslides. We generate a steady state distribution of hydrates in a 1D sediment column and then dissociate these hydrates by perturbing the sea floor conditions (i.e. change in ocean bottom temperature or sea level). We focus on the dissociation of high-concentration hydrate anomalies (i.e. lenses and nodules) at fine to coarse-grained stratigraphic boundaries that are subject to large changes in sediment permeability and cohesion over small distances. Our numerical models track the evolution of the pore-water pressure as solid hydrate anomalies decay, which can induce rapid consolidation of the sediments, and also enhance fluid flow by modifying the average density of the pore fluids. We use an infinite-slope analysis as a prelude to development of a rate and state friction approximation to quantify whether these changes in pore-water pressure or cohesion can decrease the sediment strength enough to result in immediate slope failure, or bring the system closer to failure. Our results indicate that changes in effective stress ranging from kPa to MPa are required to trigger slope failure.

Keywords: gas hydrates, hydrate dissociation, excess pore pressure, submarine landslides, hazards

NOMENCLATURE

c Athy's constant [ ]
C Cohesion [Pa]
C' Effective cohesion [Pa]
FS Factor of Safety
g Gravity [m^2 s^{-1}]
G Shear modulus [Pa]
k Permeability [m^2]
n Porosity [ ]
P_{tot} Pore fluid pressure [Pa]
P_{hydro} Hydrostatic pore fluid pressure [Pa]
P_{ex} Excess pore fluid pressure [Pa]
S_h Hydrate saturation
t time
u Darcy velocity [m s^{-1}]
W Lambert's function
x Lateral dimension of hydrate (m)
z Depth [m]
Δ Change in …
ϕ Friction angle
ϕ' Effective friction angle
δ Displacement for rate and state (m)
ξ Lateral dimension of hydrate (m)
ρ Density [kg m^{-3}]
σ' Effective stress [Pa]
σ_h Stress supported by hydrate [Pa]

μ Fluid viscosity [Pa s]
Π Thermomolecular Coefficient
ν Poisson Ratio [ ]
τ Shear stress [Pa]

Subscript
h hydrate
s sediment
f fluid
0 initial

INTRODUCTION

Submarine landslides are a natural part of the marine sedimentary system and are ubiquitous on both active and passive continental margins [1-3]. Clear evidence is recorded in coastal sediments worldwide that past changes in environmental conditions have caused hydrates to become unstable and potentially trigger submarine landslides [4]. The direct hazards posed by such events can generate tsunamis, damage infrastructure (e.g., oil platforms, telecommunication lines), and if they occur within or beneath the methane hydrate stability zone (MHSZ) cause catastrophic release of methane to the ocean and atmosphere [5].

Numerous factors can lead to slope failure by either increasing the shear stress or decreasing the shear strength – typically by reducing the effective stress, but also potentially by reducing cohesion or the effective coefficient of friction. Factors that contribute to slope failure are often separated into two categories; 1) preconditioning factors and 2) triggers [3, 6-7]. Sediments may be preconditioned for failure from their inherent characteristics (e.g., porosity, pore pressure, permeability structure) and stress histories. There are a variety of potential landslide triggers but the best recognized are earthquakes, tectonic uplift, rapid sedimentation, storm waves, anthropogenic influence, and potentially the dissociation of methane hydrates [3, 6-9].

A prerequisite for slope failure is the development and maintenance of elevated pore pressures. Several past studies have quantified excess pore pressures generated from methane hydrate dissociation [10-12] and a number of authors have gone further and applied standard slope stability analysis techniques [4, 13-14]. Nixon and Grozic [14] used a numerical model to calculate pore pressures generated by hydrate dissociation and combined their results with the infinite slope stability criterion. Their results indicate significant reductions in slope stability that can trigger failure under many conditions. Although these model calculations are instructive and point to the importance of hydrate reservoirs for slope stability issues, they are limited in predictive capability because they follow from several limiting assumptions. In particular, they assume that 1) dissociation is complete and instantaneous, 2) hydrates are located at a uniform depth along the failure plane, 3) the failure plane is at the base of the MHSZ, 4) the soil parameters are uniform along the slope dip, and 5) the friction coefficient is independent of rate and state effects.

Xu and Germanovich [12] quantified excess pore pressures in marine sediments caused by volume expansion during methane hydrate dissociation. To initiate dissociation, they assumed changes in environmental conditions such as sea level drop, tectonic uplift, and heating of hydrate-bearing sediments. Using their theoretical approach, they found that in confined sediments hydrate dissociation generates several tens of megapascals of excess pressure, while in well-connected sediments excess pore pressure development is lower, but still significant.

Sultan et al. [4] developed a model to simulate the distribution of hydrates in sediment while taking into account the pressure, temperature, pore-water chemistry, and aspects of the pore-size distribution in the MHSZ. Their model quantifies the excess pore pressure during hydrate dissociation and, unlike Nixon and Grozic [14], does not assume dissociation and slope failure necessarily occur at the bottom of the MHSZ. They use a limit-equilibrium slope-stability analysis combined with empirical data from the Storegga Slide, offshore Norway – one of the largest submarine landslides ever identified. Although a number of alternative mechanisms have been suggested (earthquakes, glacial sedimentation), they conclude that the dissociation of hydrates was the likely cause of the Storegga event.

Recently, Viesca and Rice [15-16] introduced models for submarine slope behavior that treat slide nucleation as a frictional instability that operates according to the same physical principles as identified in laboratory rock-friction

experiments that are designed to probe the nucleation of earthquakes (e.g. [17]). In either geologic setting, whether along a fault or a landslide surface, for nucleation to be possible the frictional resistance must decrease as the rate of sliding (or the slip distance) increases – behavior commonly referred to as rate-weakening (or slip-weakening). With rate-weakening friction, infinitesimal perturbations to the slip rate grow to the point where inertial effects are important (i.e. landslides) only if the slipping patch exceeds a finite and predictable size that depends on the frictional properties and effective stress. Once rapid sliding does take place, significant heat can be generated, with further feedbacks on the resisting strength as a result of the pressurization and generation of new pore fluids [18-19].

Here, we outline a 1-D numerical model that we are developing to calculate hydrate dissociation and changes in effective stress within the MHSZ. We perform slope stability analyses using the infinite-slope approximation as a prelude to development of a rate and state friction approximation. We use parameters consistent with those measured and inferred from contemporary natural hydrate reservoirs (e.g. Hydrate Ridge, offshore Oregon, USA). First, we generate a heterogeneous distribution (i.e. hydrate anomalies) of gas hydrates using a model from Rempel [20]. Rempel's [20] model predicts high-concentration hydrate anomalies that occur along stratigraphic boundaries due to changes in solubility. We induce hydrate dissociation by perturbing the equilibrium conditions via changes in the temperature and/or the pressure at the seafloor. The dissociation of high-concentration hydrate anomalies at fine to coarse-grained stratigraphic boundaries are of particular interest because they involve abrupt changes in saturation level over short distances where segregated, lens-like deposits and nodules push the sediment particles apart in order to grow, and also because they are associated with large changes in sediment permeability and strength. Our numerical models track the evolution of the pore-water pressure as solid hydrate anomalies decay to lower the cohesion of sediments, decrease the friction angle, consolidate, and alter the average density of the fluids that they contain. We hypothesize that rapid consolidation of sediment will generate excess pore pressure that will significantly reduce material strength and that enhanced fluid flow resulting from changes in the average density of the pore fluids will also weaken sediment.

MODELING STABLE HYDRATES IN A 1D SEDIMENT COLUMN

Hydrate Distribution

Hydrates typically occupy 1 to 50 % of the pore space in marine sediments [20-22]. The distribution of hydrates is controlled by the supply of gas and the local phase equilibrium conditions, both of which are modulated by sediment properties such as permeability and pore size. Empirical data (i.e. acoustic imaging and chemical analysis) and numerical modeling show that the hydrate distribution within a sediment column is heterogeneous and has "spikes" (high concentrations) and "holes" (low concentrations) at stratigraphic boundaries [20-22]. In order to properly quantify the effects of hydrate dissociation, the distribution of hydrates within the pore space must be known.

Within most of the hydrate stability zone, two-phase equilibrium is achieved between solid hydrate and an aqueous solution that contains dissolved gas. Where hydrate is present, the dissolved gas concentration is assumed equivalent to its solubility. The surface energy of the hydrate-liquid interface gives rise to "capillary effects" that result in an increased solubility where the interface is highly curved, as in the throats of small pores. The "wetting" properties of hydrate and mineral particles also enable thin aqueous films to separate these solids along pore walls. Because of these wetting and surface-energy interactions, the gas solubility is higher in more fine-grained sediments and it also increases in a given sediment as the hydrate saturation level increases (i.e. the fraction of the pore space that contains solid hydrate), which reduces the thickness of aqueous films on pore walls and increases the radii of curvature of hydrate crystal surfaces that are comparatively distant from mineral particles. At boundaries that separate sediments with different pore-size distributions, these microscale perturbations to the phase behavior enable hydrate to grow in the more coarse-grained fraction while the gas concentration is still lower than its equilibrium solubility in the adjacent fine-grained sediments. The net result is the development of large-amplitude, narrow (m-

scale or less) spikes in hydrate saturation level adjacent to hydrate-free holes. Gas transport supplies the growth of spikes by advection with the moving pore fluid and dispersive transport down the concentration gradient [20].

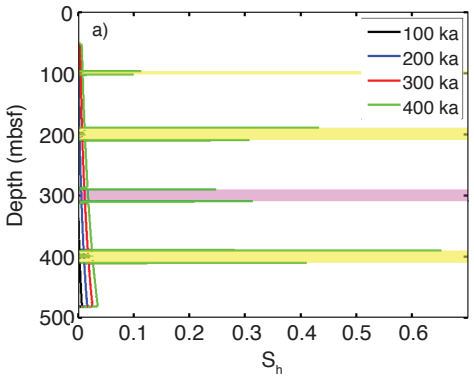

Figure 1. Predicted hydrate saturation in a sediment column. Modified from Rempel [20].

Effective Stress and Porosity

Once the hydrate spikes interconnect to distances greater than the characteristic pore size, the hydrate skeleton is able to transmit the overburden load, which reduces the local effective stress and prevents normal consolidation of the sediment [20]. For hydrate-bearing sediment the effective stress increases with depth according to

$$\frac{\partial \sigma'}{\partial z} = (1-n)(\rho_s - \rho_f)g + (1-n)\frac{\mu}{k}u + \frac{\partial \sigma_h}{\partial z} \quad (1)$$

where the first term on the right accounts for buoyancy, the second term accounts for the fluid flow (i.e. nonhydrostatic), and the third term accounts for the stress gradient transmitted between the hydrate and pore-matrix. The magnitude of the load transmitted by hydrate depends on S_h and the thermomolecular coefficient, Π, which is a measure of the hydrate-particle repulsive interactions [20]. Figure 2 shows an example of the calculated reduction in effective stress due to a hydrate spike.

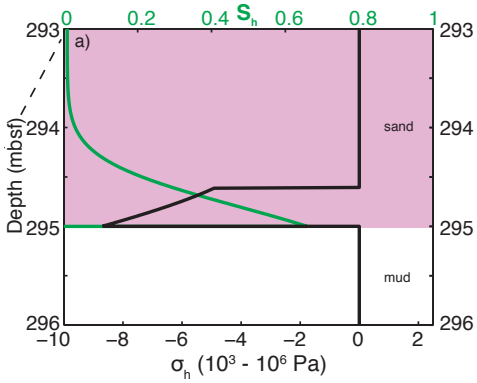

Figure 2. Close up view of hydrate anomaly. Hydrate is able to transmit load and reduce effective stress. Pink shaded areas correspond to the location of hydrate anomalies in Figure 1. Modified from Rempel [20].

Next we define sediment porosity as a function of effective stress [23]

$$n = -W\left\{-\exp\left[\frac{-b\sigma'}{g(\rho_s - \rho_f)}\right] + \ln n_0 - n_0\right\} \quad (2)$$

Combining equations (1) and (2) we can predict evolution of the sediment porosity in a hydrate bearing sediment column. We solve for effective stress and porosity for a sediment column with and without hydrates.

Excess Pore Pressure

In our model, excess pore pressure (i.e. nonhydrostatic) is generated due to consolidation and from fluid flow driven by changes in the average pore fluid density as hydrates dissociate. We use consolidation parameterizations fit to empirical data from consolidation tests (e.g. [24]) and a 1D consolidation model. The excess pore pressure will evolve according to

$$\frac{\partial P_{ex}}{\partial t} = D\frac{\partial^2 P_{ex}}{\partial z^2} \quad (3)$$

which is the linear pore pressure diffusion equation and $P_{tot} = P_{hydro} + P_{ex}$. P_{ex} is driven by changes in σ' as hydrate spikes decay. We also account for changes in pore fluid density.

Infinite Slope Model for Slope Stability

We begin by calculating the slope stability in a 1D sediment column that contains hydrate anomalies

using the infinite slope model. The infinite slope stability model is applicable to translational landslides with a planar shear surface that is much longer than it is deep, which can be a reasonable approximation for some submarine slopes. The analysis leads to

$$FS = \frac{C' + \sigma' \tan \phi'}{\tau} \quad (4)$$

where FS describes the ratio of shear strength to the shear stress. Because C' and □' are functions of the hydrate distribution and effective stress, we use functional relationships (e.g. $C' = f(S_h, \sigma')$) to describe the evolution of these parameters as hydrates dissociate.

Rate-and-State Model for Slope Stability

We are continuing to develop our rate-and-state formulation and presently only outline how we will proceed in future work. Treating the bulk sediment as a linear-elastic material, the perturbation to the stress along an incipient rupture surface due to displacement $\delta(\xi,t)$ between end-points $\xi = a\pm(t)$ (as set, for example, by lateral dimensions of hydrate anomalies) that are much closer together than the depth below the seafloor is [16]

$$\Delta\tau(x,t) \approx -\frac{G/(1-\nu)}{2\pi} \int_{a_-(t)}^{a_+(t)} \frac{\partial\delta(\xi,t)/\partial\xi}{x-\xi} d\xi \quad (5)$$

We are modifying the code developed by Skarbek et al. [25] to include pore pressure changes that are predicted by our hydrate dissociation models and examine the necessary conditions for slope failure

RESULTS AND DISCUSSION

Effective Stress and Porosity

Figure 3 shows the effective stress profile for hydrate-bearing sediments adjacent to hydrate-free sediments at a stratigraphic boundary. Calculations [20] demonstrate that under typical conditions, the presence of interconnected hydrates lowers the effective stress by between 10^3 and 10^6 Pa, depending on model parameters. This suggests that hydrates can support overburden ranging from a small fraction of the grain-to-grain contact to completely unloading the sediment.

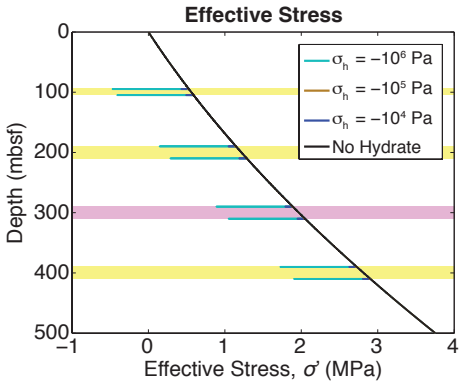

Figure 3. Effective stress along a sediment column. We allow the reduction in effective stress from hydrate anomalies to range from 10^4 to 10^6 Pa. Colored lines correspond to the stress reductions resulting from the load-bearing hydrate. Black line corresponds to the NCL. Yellow and pink shaded areas correspond to the location of hydrate anomalies in Figure 1.

Using equations (1) and (2) we find porosity increased up to 6 % from normally consolidated sediments due to load-bearing hydrate anomalies (Figure 4). This calculation assumes the largest reduction in σ', which approaches a few MPa. Deviations from the normal consolidation line (NCL) decrease with depth as the overburden increases.

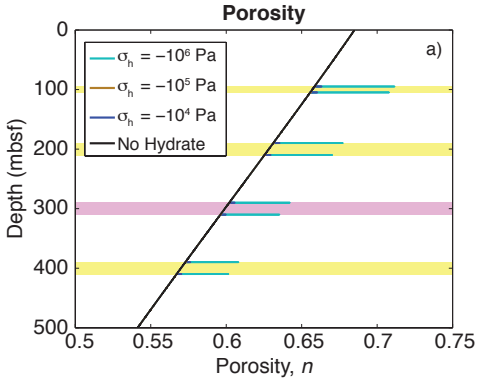

Figure 4. Predicted porosity for an under-consolidated 1D sediment column. Colored lines correspond to the stress reductions resulting from the load-bearing hydrate. Black line corresponds to the NCL. Yellow and pink shaded areas correspond to the location of hydrate anomalies in Figure 1.

Slope Stability

We quantify the slope stability for marine sediments with stable hydrates and those with dissociated hydrates. We have not yet fully coupled Rempel's [20] hydrate model with the slope stability models, so here we only describe the instantaneous dissociation of hydrates. Using the infinite slope model described by equation (4), we find that slopes are more stable if they contain stable hydrates (Figure 5). The increase in sediment strength is due to the increased cohesion and friction angle of hydrate-bearing sediments [26] that counteracts the reductions in effective stress. However, once hydrates dissociate the cohesion and friction angle return to their intrinsic values and the sediment will begin to collapse back to the NCL.

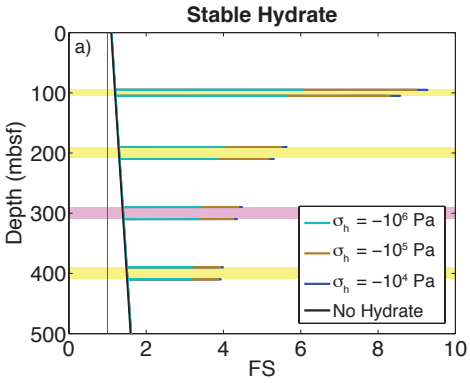

Figure 5. Factor of safety in a hydrate-bearing sediment. Colored lines correspond to the stress reductions resulting from the load-bearing hydrate. Black line corresponds to NCL. Yellow and pink shaded areas correspond to location of hydrate anomalies in Figure 1.

In addition, we calculate the slope stability of the sediments assuming instantaneous dissociation of hydrate occurs before consolidation ensues (Figure 6). Due to the increased porosity, the marine sediment is significantly weaker compared to both normally consolidated sediment and sediment with stable hydrate. However, we find that this is not enough to trigger failure and the generation of excess pore pressure is still required.

We rearrange equation (3) to calculate the P_{ex} required to initiate failure. We find that P_{ex} ranges from 10^3 to 10^6 Pa (Figure 7).

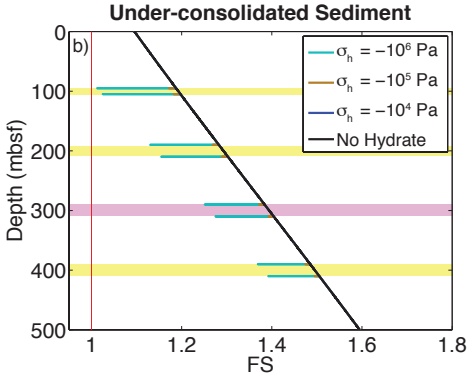

Figure 6. Factor of safety in under-consolidated sediment that no longer contains hydrate. Colored lines correspond to the stress reductions resulting from the load-bearing hydrate. Black line corresponds to NCL. Yellow and pink shaded areas correspond to location of hydrate anomalies in Figure 1.

In order to generate enough P_{ex} to trigger failure the dissociation must occur before the pressure can diffuse away from the location of the former hydrate anomaly. In other words, slope failure is expected when the timescale for consolidation following the loss of hydrate-supported pore rigidity is less than

$$\Delta t \sim \frac{z_{spike}^2 \Delta n^2 \eta}{k\beta P_{ex}^2} \qquad (6)$$

Using nominal parameters listed in Table 1 we find that Δt can range up to 10^5 years, which is much longer than the expected timescale for the dissociation of hydrates driven by a thermal or pressure perturbation.

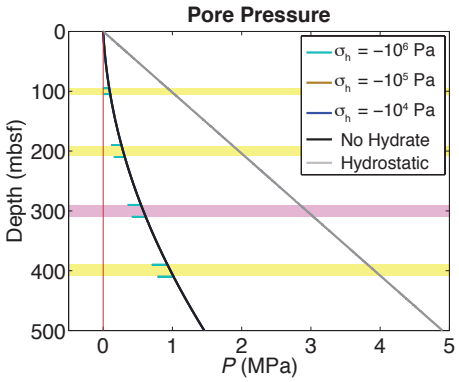

Figure 7. Black and colored lines shows the excess pore pressure required to trigger failure. Gray line indicates hydrostatic pore pressure. Yellow and pink shaded areas correspond to the location of hydrate anomalies from Figure 1.

CONCLUDING REMARKS AND FUTURE WORK

Our calculations suggest that high-concentration hydrate anomalies reduce the effective stress and prevent normal consolidation. Such hydrate spikes are expected to form at stratigraphic boundaries, where contrasts in sediment permeability and the potential for rapid consolidation increase the potential for slope instability. Using constitutive relationships between effective stress and porosity, we show that marine sediments with stable hydrates have porosity up to 6 % greater than normally consolidated sediments. Although hydrates significantly reduce the effective stress, they tend to strengthen slopes due to increased cohesion and friction angle. Once hydrate is destabilized, the sediment strength is significantly reduced due to the increased porosity. Consolidation of the sediment will generate excess pore pressure that will further weaken the marine sediment and potentially trigger slope failure. Further, quantitative predictions will be possible with the completion and coupling of a pore-consolidation model. The infinite-slope model calculations presented here are instructive and point to the importance of hydrate reservoirs for slope stability issues, but they are limited in predictive capability because they do not account for the heterogeneous distribution of strength on the slip surface that is produced by the dissociation of hydrate anomalies. Ongoing work entails the use of a rate-and-state friction formulation, which should give a more refined view by accounting for changes in frictional resistance along finite slipping patches (i.e. the size of dissociating hydrate anomalies) and the triggering produced by heterogeneous slipping as hydrate anomalies decay. This new formulation holds promise for examining how the dissociation of gas hydrates along stratigraphic boundaries can trigger and/or precondition slope failure along both passive and active continental margins.

Parameters	Value
Cohesion	
Sediment, C [Pa]	$0.03\sigma'$
Hydrate, C_h [Pa]	1.0×10^6
Friction angle	———
Sediment, Φ [°]	29
Sediment with hydrate, Φ_h [°]	40
Sediment density, ρ_s [kg m^{-3}]	2670
Water density, ρ_f [kg m^{-3}]	1000
Slope angle, θ [°]	3 - 10
Sediment depth, z [m]	500
Surface porosity, n_0 [ ]	0.685
Athy's constant, b	4.0×10^{-4}
Lambert's function, W	$We^W = x$
Hydraulic diffusivity, D [m^2 s^{-1}]	10^{-9} - 10^{-6}
Anomaly thickness, z_a [m]	10^{-1} - 10^{0}
Permeability, k [m^2]	10^{-18} - 10^{-14}
Pore compressibility, β [Pa^{-1}]	10^{-10}
Dynamic viscosity, η [Pa s]	10^{-3}

Table 1. Nominal parameter values.

REFERENCES

[1] Locat, J, and Lee HJ. Submarine landslides: advances and challenges. Canadian Geotechnical Journal 2002; 39(1): 193-212.

[2] Chaytor JD, ten Brink US, Solow AR, and Andrews BD. Size distribution of submarine landslides along the US Atlantic margin. Marine Geology 2009; 264(1): 16-27.

[3] Masson, DG, Wynn RB, and Talling PJ. Large landslides on passive continental margins: Processes, hypotheses and outstanding questions. In Submarine Mass Movements and their Consequences 2010: 153–165.

[4] Sultan N, Cochonat P, Foucher JP, and Mienert J. Effect of gas hydrates melting on seafloor slope instability. Marine Geology 2004;213(1):379–401.

[5] Nisbet EG, and Piper DJ. Giant submarine landslides. Nature 1998; 392(6674): 329-330.

[6] Mosher DC. International year of planet Earth 7. Oceans: Submarine landslides and consequent tsunamis. Canada. Geoscience Canada 2009;36(4).

[7] Mosher DC, Shimeld J, Hutchinson D, Lebedeva-Ivanova N, and Chapman CB. Submarine landslides in arctic sedimentation: Canada Basin. In Submarine Mass Movements and Their Consequences 2012;147–157.

[8] Grozic JLH. Interplay between gas hydrates and submarine slope failure. In Submarine Mass Movements and their Consequences 2010; 11–30.

[9] Owen M, Day S, and Maslin M. Late Pleistocene submarine mass movements: Occurrence and causes. Quaternary Science Reviews 2007; 26(7):958–978.

[10] Kwon TH, Cho GC, and Santamarina JC. Gas hydrate dissociation in sediments: Pressure-temperature evolution. Geochemistry, Geophysics, Geosystems, 9(3), 2008
[11] Lee JY, Santamarina JC, and Ruppel C. Volume change associated with formation and dissociation of hydrate in sediment. Geochemistry, Geophysics, Geosystems 2010; 11(3).
[12] Xu X, and Germanovich LN. Excess pore pressure resulting from methane hydrate dissociation in marine sediments: A theoretical approach. Journal of Geophysical Research: Solid Earth 2006;111(B1).
[13] Kwon TH, and Cho GC. Submarine slope failure primed and triggered by bottom water warming in oceanic hydrate-bearing deposits. Energies 2012; 5(8):2849–2873.
[14] Nixon MF, and Grozic JLH. Submarine slope failure due to gas hydrate dissociation: A preliminary quantification. Canadian Geotechnical Journal 2007;44(3):314–325.
[15] Viesca RC, and Rice JR. Modeling slope instability as shear rupture propagation in a saturated porous medium. In Submarine Mass Movements and Their Consequences 2010; 215–225.
[16] Viesca RC, and Rice JR. Nucleation of slip-weakening rupture instability in landslides by localized increase of pore pressure. Journal of Geophysical Research: Solid Earth 2012;117(B3).
[17] Marone C. Laboratory-derived friction laws and their application to seismic faulting. Annual Review of Earth and Planetary Sciences 1998; 26(1):643–696.
[18] Brantut N, Sulem J, and Schubnel A. Effect of dehydration reactions on earthquake nucleation: Stable sliding, slow transients, and unstable slip. Journal of Geophysical Research: Solid Earth 2011;116(B5).
[19] Rempel AW, and Rice JR. Thermal pressurization and onset of melting in fault zones. Journal of Geophysical Research 2006; 111(B9):B09314.
[20] Rempel AW. A model for the diffusive growth of hydrate saturation anomalies in layered sediments. Journal of Geophysical Research: Solid Earth 2011;116(B10).
[21] Trehu AM, Long PE, Torres ME, et al. Three-dimensional distribution of gas hydrate beneath southern Hydrate Ridge: constraints from ODP Leg 204. Earth and Planetary Science Letters 2004, Volume 222, Issues 3-4, 845-862, ISSN 0012-821X, DOI: 10.1016/j.epsl.2004.03.035.
[22] Bohrmann G, Torres ME. Gas Hydrates in Marine Sediments. Marine Geochemistry 2006, 481-512, DOI: 10.1007/3-540-32144-6_14
[23] Skarbek RM., and Saffer DM. Pore pressure development beneath the décollement at the Nankai subduction zone: Implications for plate boundary fault strength and sediment dewatering. Journal of Geophysical Research: Solid Earth 2009;114(B7).
[24] Tan B, Germaine JT, and Flemings PB. Data report: Consolidation and strength characteristics of sediments from ODP Site 1244, Hydrate Ridge, Cascadia continental margin. In Proc. Ocean Drill. Program Sci. Results 2006;204:1–148.
[25] Skarbek RM, Rempel AW, and Schmidt DA. Geologic heterogeneity can produce aseismic slip transients. Geophysical Research Letters 2012; 39(21).
[26] Waite WF, Santamarina JC, Cortes DD Dugan B, Espinoza DN, Germaine J,... & Yun TS. Physical properties of hydrate-bearing sediments. Reviews of Geophysics 2009;47(4).